Challenge Journal of Structural Mechanics

Research Article

Strengthening and performance assessing historical cinema hall balcony according to new Turkish Earthquake Code

Memduh Karalar [a,*], Murat Çavuşli [a]

[a] *Department of Civil Engineering, Zonguldak Bülent Ecevit University, İncivez, 67100 Zonguldak, Turkey*

ABSTRACT

Strengthening historical buildings and evaluating their performances make great contributions to both the history of the country and the tourism of the country. In this study, performance analysis and evaluations of the historical cinema hall balcony, which was built in 1933 by a French company and served to Zonguldak province for a long time, are presented in detail. This cinema hall was frequently used by local people between 1933 and 1999 and hosted many Yeşilçam movies. Firstly, examinations were performed in the historical cinema hall and the areas (columns, beams and floors) that were damaged in time were identified. According to the obtained information, it was determined that there were significant damages in the carrier system of the building and there were visible cracks and damages in the columns of the cinema hall. It was also observed that explosions occurred in one of the main carrier columns of the balcony. After the core samples taken from the balcony were tested in the laboratory, the current status of the carrier elements and reinforcements were determined with the help of an x-ray rebar scanner. After all these processes, the structure was modeled as three dimensional (3D) using a special computer program and performance evaluations were performed regarding the current state of the structure. As a result of the performance evaluation, it was determined that the balcony of the historical cinema hall could not survive anymore and would collapse over time. It was concluded that there were great damages especially on the balcony columns and a reinforcement should be made on a total of 6 columns. Strengthening was made to 4 different main columns and a performance analysis was performed again in strengthened structure. After strengthening, it was understood that the columns of the balcony of the cinema hall could survive for a long time.

ARTICLE INFO

Article history:
Received 28 July 2020
Revised 23 October 2020
Accepted 17 November 2020

Keywords:
Structural strengthening
Performance evaluation
Deflection evaluation
Column end force
Turkish Earthquake Code

1. Introduction

Turkey has a very ancient history and many empires that have witnessed this history have left deep traces and historical heritages in this country. It is seen that there are many building types in this historical heritage, from wooden structures with excellent architecture to reinforced concrete structures built thousands of years ago. The protection and reuse of these historical buildings make great contributions to the economy and tourism of our country. Nowadays, studies on the protection of historical buildings have become widespread. The main purpose of strengthening and preserving historical constructions is to ensure surviving of these structures for a long time. However, while performing these vital operations, it should be essential to keep the historical texture of the historical building. Recently, historical structures in Turkey are faced with strong ground movements such as earthquakes, floods and negative threats of rapid urbanization that has occurred.

While Turkey can protect the large-scale public structures, small-scale structures, most of which are privately owned, cannot adequately protect due to the lack of legal infrastructure. For this reason, many historical buildings

* *Corresponding author*. Tel.: +90-372-291-2582 ; Fax: +90-372-257-4023 ; E-mail address: memduhkaralar@beun.edu.tr (M. Karalar)
ISSN: 2149-8024 / DOI: https://doi.org/10.20528/cjsmec.2021.01.004

have been demolished recently. However, these structures could have been used for both local people and country tourism for a long time by performing earthquake evaluation of structures. The strength of a historical building depends on the structural system, the geometry of the building and the mechanical properties of building. For this reason, different structural deformations and defeats can occur under constant loads in similar historical buildings. The main causes of the defeats in historical buildings are the loads caused by the building's own weight, loads caused by ground vibrations and other natural disasters. However, it is very rare situation that a historical building destroyed or damaged due to its own weight. The main reason for the damage or demolition of historical buildings are natural external loads, man-made artificial loads or structural problems due to other environmental effects (Örmecioğlu, 2010). In the literature, the studies on the strengthening and reuse of historical structures are summarized as follows: In a study, it has been performed strengthening of the walls, domes, vaults and foundations with injection resins and anchorage systems. In this study, it is stated that the compressive and shear strength of resins are very high. Moreover, it was observed that the reaction time of said resins ranged from 30 to 180 seconds. It has been stated that Carbopur WF resin does not swell voluntarily in anhydrous environment and its compressive strength reaches around 800 kg/cm2 in a few minutes. It is stated that Carbopur S resin swells 100-200% in anhydrous environment and its compressive strength is around 100-300 kg/cm2 in a few minutes. It is shown that two component resins have swelling and foaming rate of 2-6 in free environments (such as direct contact with air). However, it is stated that their swelling rates in environments such as concrete and ground are between 1.0-2.5. The tensile, torsional and compressive strengths of these resins have been proved to be very high (Kasapgil, 2007). In addition, the strengthening was carried out in Adana Ulucami minaret in 2007. Separated and broken stones and cracks in Adana Ulucami Tower are filled with resins that adhere well. With this filling process, the stones are prevented from cracking due to expansion, water leaking into the cracks, washing the material inside and expanding the cracks (Kasapgil, 2007). Later, a study was carried out on the repair and strengthening of the Ahi Celebi Mosque. In this study, the repair and strengthening methods of masonry domes damaged due to effects such as vertical loads, support collapse, earthquake, and the effectiveness of the pull circle formed in the support area are given with the application example of Ahi Çelebi Mosque. The structure is modeled using SAP2000 software under the influence of vertical and earthquake loads. The application of the pull-out circle led to a significant reduction in the tensile stresses formed in the dome (Sesigür and Çelik, 2007). In addition, a building was proposed to be demolished and reconstructed by technical teams. The building is located only 7.5 km from the Arifiye fault zone torn in the 1999 East Marmara Earthquake. As a result of this study, a strengthening and repair project of the building was made and the building was opened eight months after the earthquake. The behavior curve of the structure (bottom shear force - peak displacement) remained at the “immediate use” level (Arioglu et al., 2007). Moreover, a study on the pre-fire condition of Urla Old Monopoly Building (Arditi Pavilion) and the strengthening of the building was carried out. Although the outer walls of the building were standing before the fire, it was determined that there were collapses and decays in the building (Aydın et al., 2015). In a study, structural analyses were carried out within the scope of restorations of historical bridges and their results are presented in detail. It has been proved that in cases where the said research is not done / insufficient, the damage can occur again after the restoration. It has been stated that the determinations related to the building and the ground are important in terms of supporting the carrier systems of the historical bridges (Sert and Partal, 2015). The dynamic behavior of the scaled stone arch bridge model was examined experimentally and analytically. In this study, the dynamic behavior of the 1/10 scale model of a stone arch bridge, which is frequently encountered in applications, was investigated experimentally. The first six frequencies, mode shape and modal damping rate of the model, which was carried out using the environmental vibration test, were determined. In order not to damage the model during the measurement, the bridge behavior was determined with uniaxial seismic accelerometers under the vibrations coming from the environment without using additional vibrators. Dynamic characteristics were determined analytically by performing modal analysis on the model created using three-dimensional solid elements in the SAP2000 program. At the end of the study, experimental dynamic characteristics and analytical results were compared and differences were revealed (Türker et al., 2015). Then, a study was presented the restoration-conservation of historical Malabadi Bridge. Restoration-conservation carried out by the General Directorate of Highways between 2009-2013 on the Historical Malabadi Bridge, which was built in the Artuqid Period on the Batman Water in Diyarbakır province (Sert and Yılmaz, 2015). Linear and nonlinear seismic analyzes of the historical Tağar Bridge on Tağar stream in Çemişgezek district of Tunceli province were performed. For this purpose, the bridge is modeled with three dimensional finite elements. Acceleration records of the Erzincan earthquake were considered as seismic effects. ANSYS finite element program was used in the analysis (Onat and Sayın, 2015). A study has been carried out on structural system features, damages, repair and strengthening techniques in historical buildings. In the study, information is given about how the concept of protection is perceived from past to present and what steps are taken, types of historical buildings, materials and properties used in historical buildings. In addition, detailed information about carrier system constituting the historical structure, damages occurring in these structures and damage determination methods applied today, the examination of earthquake safety within the framework of the conditions specified in the earthquake regulation of masonry buildings and the repair and strengthening techniques applied in historical buildings are presented (Mahrebel, 2006). In another study, seismic performance evaluation of a historical wall structure

was performed. The building performance was made by comparing the old and new Turkish earthquake standards. Non-destructive experimental measurement methods have been used to obtain reliable results in seismic performance evaluation. As a result of the analyzes, maximum displacements and basic stresses were obtained. In terms of displacement control, the structure showed only limited damage during the earthquake recording applied. In other word, the building behaved linearly when it was exposed to the selected earthquake (Günaydın, 2019). New Zealand is a country famous for its historical structures and the protection of the historical texture is vital for this country. In a study, performance assessment of historical buildings in a city in New Zealand was made. Using the MCDA methodology, the performance of historical buildings was revealed and suggestions were made (Aigwi et al., 2019). Performance-based assessment has recently become crucial for multi-story, non-reinforced walled buildings. However, it is very difficult to evaluate the performance of multi-storey historical buildings due to their complex engineering features and structural performances. In a study, the historical scribe school in Erzurum was selected for performance analysis, and the seismic weaknesses of this historical building were identified and its structural performance was evaluated (Korkmaz et al., 2018). It is vital to protect the historical heritage against horizontal loads (such as earthquakes) and to examine these structures in three dimensions. In a study, the earthquake performance of three different damaged palace walls in Mantua (Northern Italy) after the 2012 Emilia earthquake was investigated. Three different palace structures are modeled in three dimensions and the material parameters are laid out in detail. Comparison between three-dimensional numerical results and damage research has shown that the numerical approach used in this study may be an adequate tool to accurately assess the seismic response of historic structures (Valente and Milani, 2019). In the construction of historical buildings, only static loads are generally taken into account. Therefore, these structures can be damaged or destroyed due to seismic effects. Earthquake performances of historical buildings should be obtained in order to move them to the future and protect them. In a study, the nonlinear seismic responses of the Malabadi Bridge built in the 12th century were evaluated. To determine the material properties of the bridge, uniaxial compressive strength tests, ultrasound tests, Schmidt hammer tests and mass loss tests were performed. It was observed that there was no damage zone on the arches and spandrel walls under D1 and D2 earthquake loads and plastic deformations occurred in the filling material under D2 earthquake loads. Numerical results showed that the main arch of the bridge was heavily damaged under the earthquake load D3 (Karaton et al., 2017). Historical buildings are often vulnerable to earthquake damage throughout their lifetimes, and strengthening is needed to survive these structures. This strengthening process is handled through analysis considering the current state of the buildings. However, there are few studies focusing on the strengthening methods applied. In a study, the structural behavior of conditions before and after the strengthening of a historical structure was investigated. In order to compare the conditions, theoretical finite element models were developed and then experimental analysis of the historical building was performed. The results show that the strength of the reinforced structure increased 3 times compared to the initial state (Ercan, 2018). In another study, in the east of Turkey on October 23, 2015 during the main shock of the Van earthquake damage in two historic buildings partially collapsed was investigated. The solid body of both structures survived without earthquake damage, but the Narthex of both structures collapsed. First, the existing standards (ASCE 41, 2006; EC8-3, 2005; PERPETUATE, 2010) were extensively studied. Then, response spectrum analyzes were performed to evaluate the seismic performance of the structures. According to the results of the numerical analysis, the causes of the collapse of the building were revealed (Cakir et al., 2015). Finally, in a study, an algorithm was developed to determine the failure loads of single span circular masonry arch bridges according to the lower-limit theorem of limit analysis. The algorithm uses linear programming techniques and converges at the bottom of the true burden load value, that is, on the safe side. The algorithm is programmed in Matlab environment (Orhan and Özyazıcıoğlu 2015).

As can be seen from the studies in the literature, there are many studies on historical structures in the past. However, there is no study on the strengthening of movie theaters, which are important for tourism and a place frequently used by the public, by taking into consideration the 2018 Turkish earthquake regulation and earthquake performance. The aim of this study is to perform earthquake strengthening and to evaluate the earthquake performances in order to survive of the historical movie theater, which is important for the country's tourism, for a long time. For this purpose, the historical cinema hall built in 1933 was selected for analysis and evaluations. This movie theater is very important for Zonguldak and our country's tourism and it is vital to extend the life of this building. For this reason, this study contributes significantly to the literature and country tourism.

2. Material and Method

In this study, the incremental single-mode push (pushover) analysis method was used for performance evaluations. This method impacts the calculated horizontal loads on the system, taking into account a predetermined distribution. The structure is increased step by step up to a certain limit value with these imposed loads and the carrier system elements are brought to capacity. This limit value can occur in two ways. It occurs when the lateral stability of the carrier system is degraded or the horizontal displacement value that brings the structure to the mechanism state is reached. In incremental single-mode propulsion analysis, in each step, internal forces, displacements and plastic deformations in the carrier system elements are calculated. Accordingly, the curve that gives the relationship between the base shear force and the peak displacement of the structure, that is, the pushover curve, is determined. In addition, building

performance evaluations have been performed considering the 2018 Turkish New Earthquake Regulation. In the current status of the building, there are major damages and explosion in the balcony columns. In addition, there are deflections in the existing balcony beams. Most of the balcony flooring reinforcements have come out and are corroded. In this study, first of all, the relievo of the historical movie theater was obtained in detail. Because this building is a historical monument building, no project or technical knowledge of this structure was available. Each carrier element is determined in detail and the length information of each carrier is entered in detail in the AUTOCAD program. Due to the fact that the balcony flooring is inclined and variable thickness, very sensitive measurement has been taken and sensitivity has been shown while removing the leveling. Then, information was obtained about the current status of the fittings in the carrier elements using an x-ray device. Concrete X-ray scanning has been in use for a long time in the construction industry due to its accuracy. By using this device, information was obtained about the current state of the reinforcements in the concrete and it was observed that most of the reinforcement was corroded. 3D model of the building, which was removed, was created with the help of the IDECAD static program. IDECAD program is used finite element method while 3D modelling and 3D analyzing of structures. All carrier elements are carefully entered into the program and balcony flooring has been created in accordance with the project. Finally, core samples were taken from bearing columns supporting the balcony flooring, bearing beams and flooring. While taking the core sample, due to the historical feature of the building, care was taken not to damage the building too much. Moreover, while testing cylinder samples, initial speed, dimensions (diameter, height) defined to device. Core samples were experimentally pressure tested and their mechanical properties were determined. After the concrete samples were tested in the test device, information about the current concrete quality in the structure was acquired. The material parameters of all carriers are carefully determined to program. Young's modulus, Poisson ratio, shear modulus is defined to IDECAD program to obtain more realistic analysis results of structure. In addition, the structure is divided into equal parts and mesh process has been made. During the meshing process, all the elements of the structure are divided into equal pieces of approximately 10 cm. The analyzes were first made by considering the current state of the building. Balcony columns and beams were evaluated for G+Q+E (X and Y) combinations according to 2018 earth-quake regulation. These standard combinations were used to obtain the most critical condition of the historical building during the earthquake. These combinations show the situation in which the structure receives the greatest moment and shear forces. Therefore, these combinations were used in this study. According to the results of the analysis, it was observed that the building had more difficulty in surviving and that earthquake reinforcement was essential. The carrier elements that need reinforcement were determined by examining the results in detail and reinforcement jacketing was performed on these carrier walls. During jacketing, care was taken not to damage the historical building too much. When the reinforced structure was analyzed again, it was seen that the cinema hall could remain standing for many years as a result of the jacketing, and the building was provided to contribute to the tourism and national economy for many years.

3. General Information about Historical Cinema Hall

After the proclamation of the republic, Zonguldak province became a province where large investments were made in tourism and economy. As a result of the investment of businessmen, Zonguldak has become one of the provinces with the highest population in Turkey. The historical cinema hall, which is the subject of this study, was built in Zonguldak Center after the proclamation of the Republic in 1933 and served as a community center for the tourism of our country and the people of Zonguldak for a very long time. The building, which served as a community center until 1951, continued to serve as a cinema and theater hall after 1951. This historical structure is one of the largest historical heritages left to Zonguldak after the proclamation of the Republic (Fig. 1).

Fig. 1. Views of Zonguldak historical theater hall (1965).

After 1951, many Yeşilçam artists watched films in this building and thousands of films were screened. At that time, what movies were on display (cowboy movies, adventure movies, crime) were first seen in this cinema. Even the 1974 world cup documentary was released in this cinema. But over time, the effectiveness of the population of the province of Zonguldak institutions were put dwindled, Turkey's most populous cities in between is between the least populated provinces. For this reason, interest in tourism and cultural events has decreased over time and these historical cinema structures have been abandoned to their fate. In 2013, this building was completely closed and local people were deprived of the cinema viewing activity in this historical building.

4. Material Parameters of Historical Cinema Hall and Modeling Three Dimensions

Since 1933, no interference (strengthening) has been carried on the carriers of the historical movie theater subject to this study. For this reason, it has been determined that the building is sufficiently tired and the modification of the structure is needed in order to survive longer. This structure is a reinforced concrete structure and the using of ribbed reinforcement in the building in 1933 is an indicator of the value given to the buildings and people at that time. In the building, there are beams with a thickness of about 1 meter and all of their floors are made of reinforced concrete. The lowest floor is the ground floor and at that time this floor was used as an entrance to the cinema and the place where the stage was placed. Ground floor and first floor plans are the same. But the slope of the balcony flooring on the 1st floor is very different from the ground floor. 1st floor balcony floor has 12% slope. The plans of the building before and after strengthening are presented in Figs. 2 and 3.

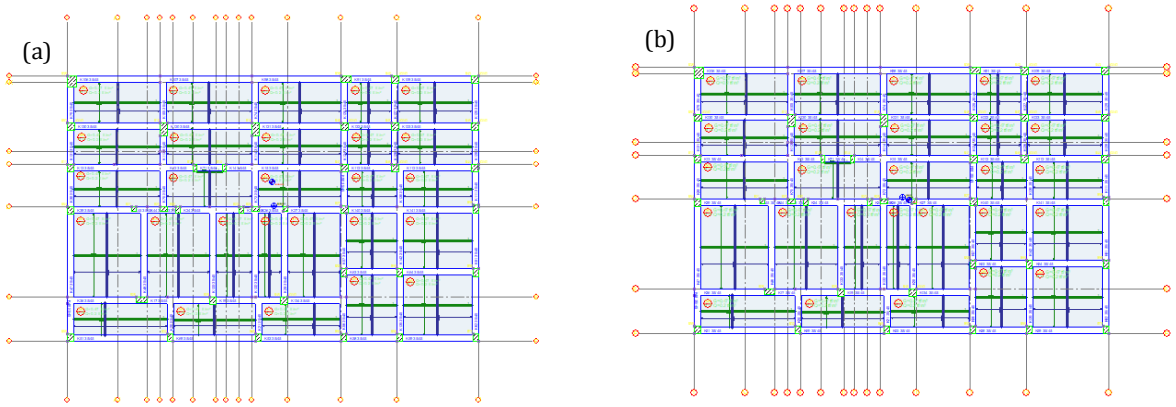

Fig. 2. Structure plan before reinforcement: (a) Ground floor; (b) 1st floor.

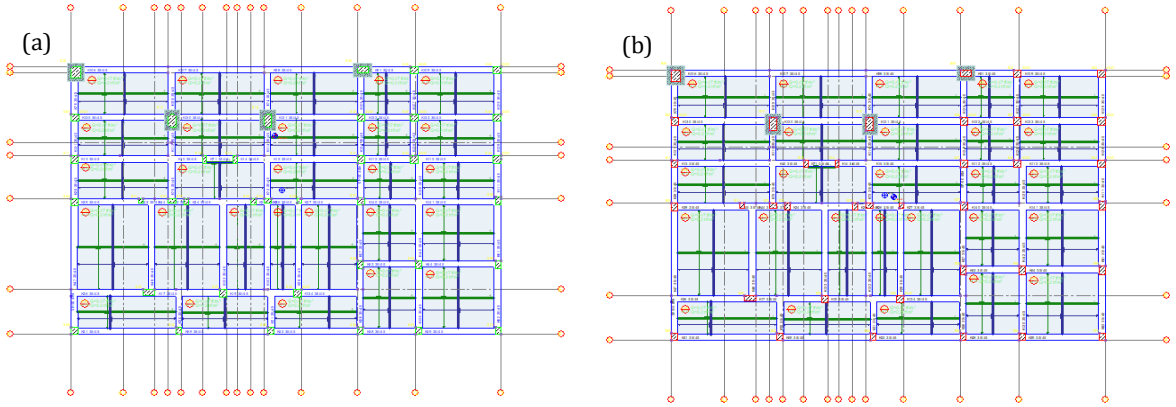

Fig. 3. Structure plan after reinforcement: (a) Ground floor; (b) 1st floor.

In this study, core samples were taken from the carrier elements of the building and the balcony floor. Due to the fact that the building is a historical building, care was taken not to damage the historical artifact while taking the core sample. Three samples were taken from each carrier and these samples were subjected to pressure testing in the laboratory (Fig. 4). According to the pressure test results, in some of the balcony main columns (S39, S40, S41, S42), concrete class has been determined as C14 and all other carriers have been determined as concrete class C18. Then all the carrier elements were scanned with an x-ray device and the current state of the reinforcements in it was determined (Fig. 5). It was determined that most of the reinforcements were corroded and it was observed that melts and explosions occurred in the reinforcements over time in both main bearing columns of the balcony. After all these operations were done, all geometric and mechanical properties of the building were entered into the IDECAD static program. First, the current state of the building was modeled, and after analyzing, some damaged parts of the building were reinforced. The existing modeled and reinforced state of the building are presented in Figs. 6 and 7. Moreover, moment-rotation relationship was obtained for main column (S41) of balcony of historical structure by using XTRACT program (Fig. 8). Finally, a performance objective may include consideration of damage states for several levels of ground motion and would then be termed a dual or multiple-level performance objective. Based on performance objective the capacity and demand curve is drawn and based on it the suitable design is chosen for 3D analyses (Fig. 9). Moreover, jacketing detail of S41 column is shown in Fig. 10.

Fig. 4. Core samples taken from the structure:
(a) Main column S41; (b) Main column S42; (c) Balcony flooring.

Fig. 5. Examination of carrier elements with X-ray device.

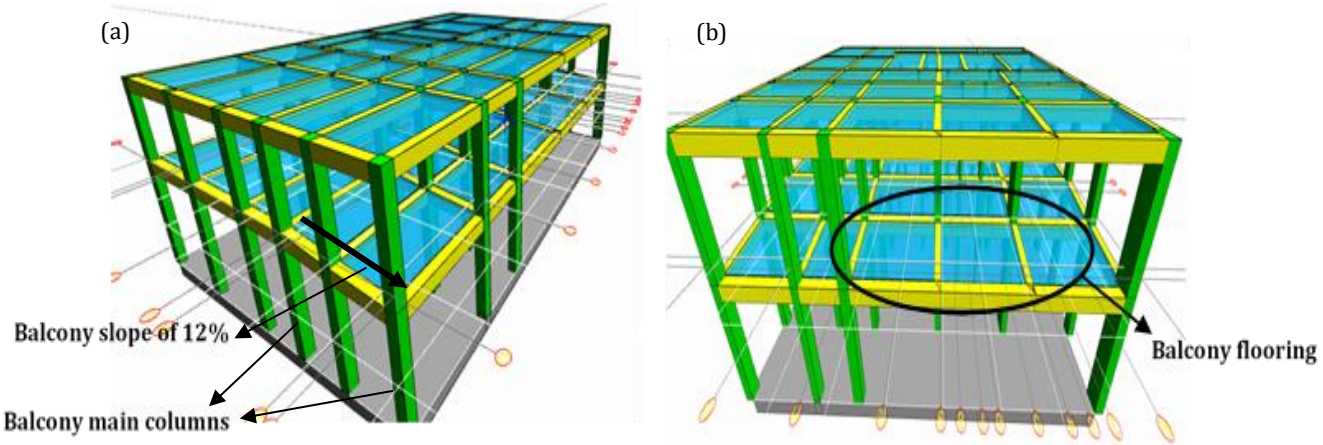

Fig. 6. Three-dimensional view of the building before reinforcement: (a) Right view; (b) Front view.

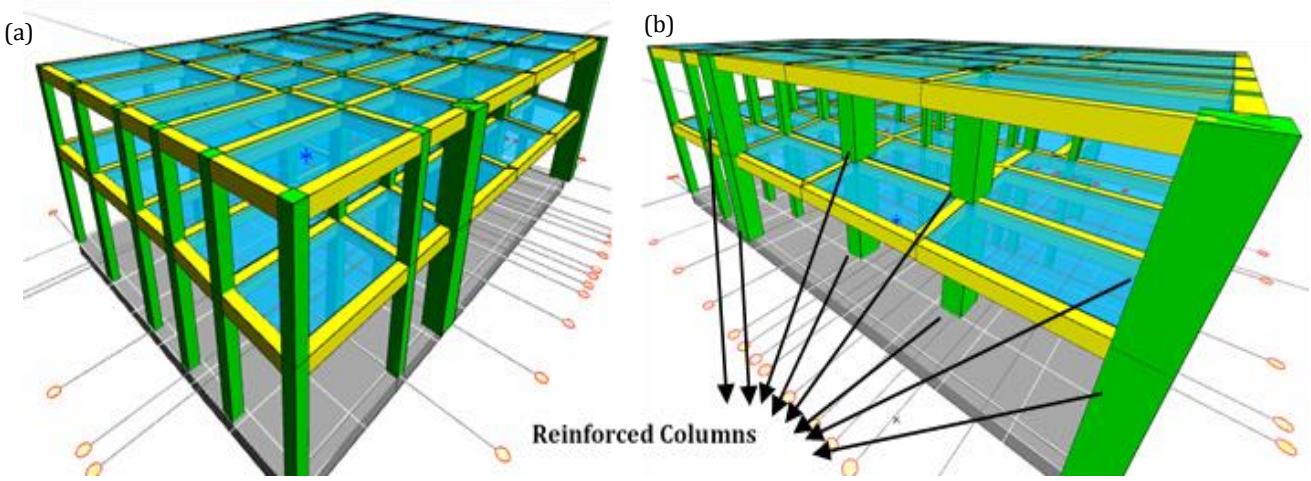

Fig. 7. Three-dimensional view of the building after reinforcement: (a) Right view; (b) Left view.

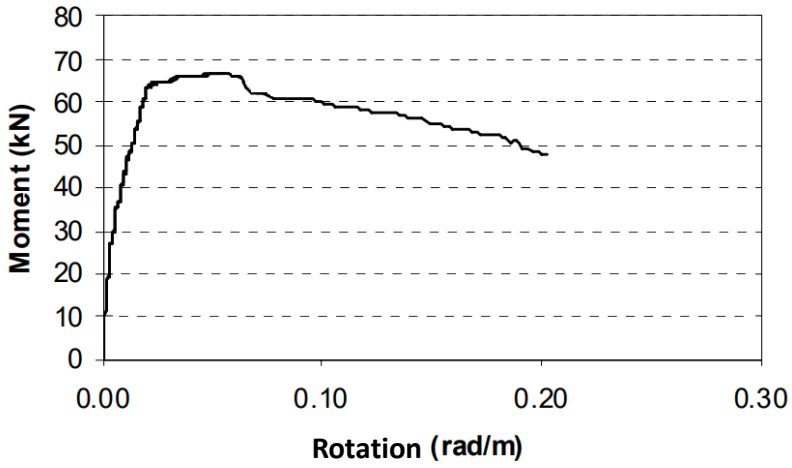

Fig. 8. Moment-rotation relationship for main column of balcony of RC structure.

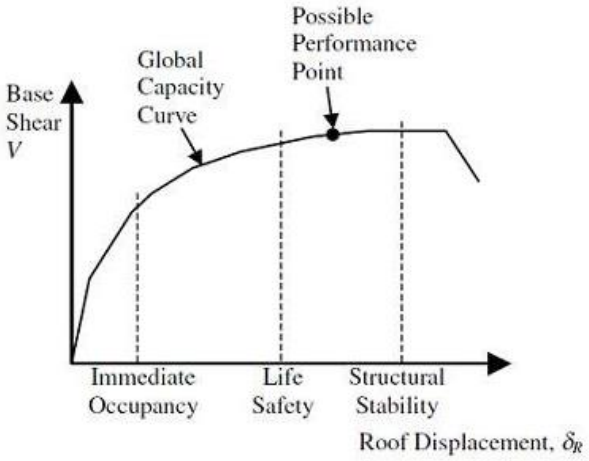

Fig. 9. Capacity curve of structure.

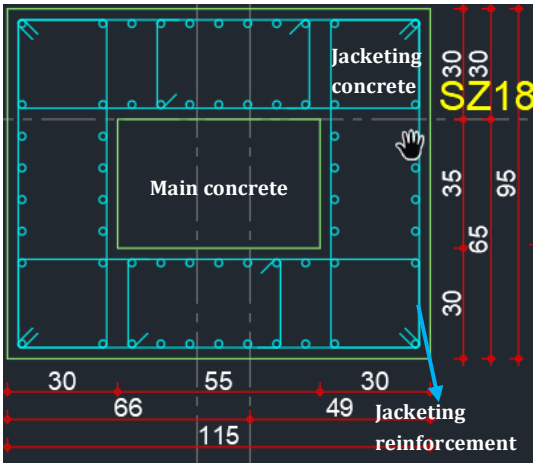

Fig. 10. Jacketing detail of S41 column.

5. Results and Discussions

In this section, the before and after conditions of Zonguldak historical movie theater balcony are evaluated and compared with each other. Firstly, the current situation of the building is taken into consideration and a performance evaluation is performed for current situation of building. As a result of this evaluation, damaged carrier elements of the building were identified. According to the results of the analysis, it was seen that damages occurred on the balcony floor and columns and it was thought that this balcony could be demolished in a

short time. The carrier elements detected later were reinforced with jacketing. A total of 4 columns on the ground floor and 4 columns on the first floor were jacketed. The jacket thickness is 20 cm and C25 concrete was used when jacketing. A total of 4 columns and 3 balcony beams were examined both before and after reinforcement and presented in this section. These columns and beams are presented in Fig. 11. In this study, balcony columns and beams were evaluated for G+Q+E (X and Y) combinations according to 2018 earthquake regulation. These standard combinations were used to obtain the most critical condition of the historical building during the earthquake. These combinations show the situation in which the structure receives the greatest moment and shear forces. Therefore, these combinations were used in this study.

5.1. Analysis results for the current situation of the building

Analysis results for damaged columns and beams of Zonguldak historical movie theater balcony are presented in this section as table and graphically. Identified balcony columns were named as S39, S40, S41 and S42. In addition, the weak balcony beams are named as KZ1, KZ2 and KZ3 (Fig. 11). According to the G+Q+E (X and Y) combination, the loads occurred on the existing columns and beams of the building are given in Tables 1-7. Besides, force charts for reinforced situation of this structure are presented in Tables 8-14. In Table 1, the end forces of S40 column for 8 different load combinations are shown in detail. When these forces are examined, the maximum normal force in *i* direction is -21.7 kN and this force was obtained in G + Q + EY combination. Moreover, the maximum normal force in *j* direction is 18.5 kN. When the largest shear forces occurred in S40 column are examined, the largest shear force obtained in *i* direction is 3.87 kN. When the largest shear forces in *j* direction are examined, it is observed that 4.44 kN occurred for G+Q+EX combination. When the biggest moment values in *i* direction are examined, the biggest moment occurred in S40 column is obtained in G+Q+EX combination and this moment value is 7.89 kNm. In addition, the greatest moment value in *j* direction is 6.76 kNm (Table 1). When these values are examined, it is determined that very big forces and moments are on the S40 column.

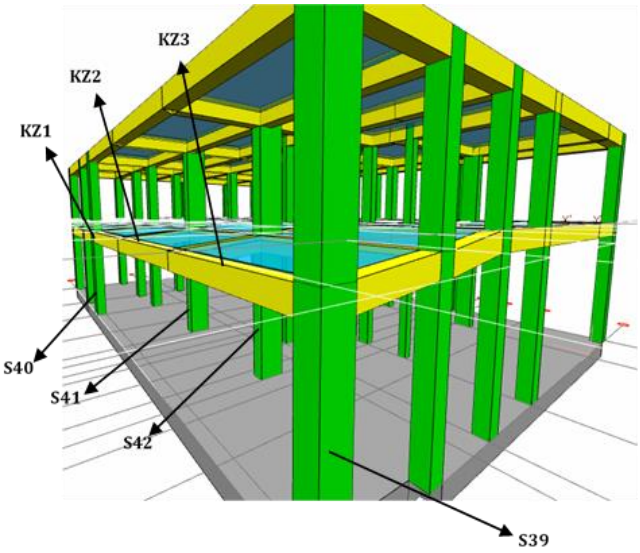

Fig. 11. The most critical sections for the current situation of the building.

Table 1. End forces for S40 column.

Load	Ni	V2i	V3i	M2i	M3i	Nj	V2j	V3j	M2j	M3j
Unit	kN	kN	kN	kNm	kNm	kN	kN	kN	kNm	kNm
G+Q+EX1	-14.5025	3.8774	0.1412	1.0019	7.8907	10.9293	4.4465	0.0424	0.8112	6.7651
G+Q+EX2	-14.9606	3.6124	0.2147	1.151	7.3354	11.2831	4.1399	-0.0117	0.8255	6.3374
G+Q+EY1	-21.0659	1.0628	1.2323	2.5222	3.711	15.6528	1.837	-0.5852	1.1936	3.5332
G+Q+EY2	-21.7739	0.6313	1.3573	2.7769	-1.2605	16.1889	1.3439	-0.6745	1.2251	0.2736
G+Q-EX1	-21.625	-2.6017	0.0827	-0.589	-6.1615	18.5192	-1.9367	0.0337	0.3868	-3.9555
G+Q-EX2	-21.1669	-2.3367	0.0092	-0.7381	-5.6062	18.1654	-1.6301	0.0878	0.3725	-3.5278
G+Q-EY1	-15.0616	0.2129	-1.0084	-2.1093	-1.9818	13.7958	0.6728	0.6613	0.0044	-0.7236
G+Q-EY2	-14.3537	0.6444	-1.1335	-2.364	2.9897	13.2596	1.1659	0.7506	-0.027	3.0832

It was determined as a result of on-site examinations that the explosions occurred in S39 column over time. According to performance analysis results, it was observed that the greatest moments and forces occurred in this column. The greatest normal force occurred in S39 column is -26.21kN in *i* direction and -10.23 kN in *j* direction. In addition, the largest shear force took place in this column is -5.58 kN in *i* direction and -2.98 kN in *j* direction, and these forces occurred in G+Q+EY combination. The biggest moments in this column are 11.33 kNm in *i* direction and -5.89 kNm in *j* direction (Table 2). When these values are evaluated, it is observed that larger loads and moments occurred in the S39 column when compared with S40 column and it was observed that more damage occurred in the S39 column.

S41 column is a column that is more inward than other columns. In Table 3, the end forces are presented considering the 8 different combinations for S41 column. The biggest normal force on this column is -52.8 kN, and this force was obtained in G+Q+EY combination in *i* direction. The largest shear force in *i* direction is 6.08 kN and the largest moment value in the same direction is

14.4 kNm. In *j* direction, the largest normal force is 3.2 kN. The largest shear force in the same direction is -0.16 kN. The maximum momentum value on this column is 0.0034 kNm. According to these values, the normal force, shear force in *i* direction are much more than *j* direction.

Table 2. End forces for S39 column.

Load	Ni	V2i	V3i	M2i	M3i	Nj	V2j	V3j	M2j	M3j
Unit	kN	kN	kN	kNm	kNm	kN	kN	kN	kNm	kNm
G+Q+EX1	-17.6446	-0.4132	2.3935	7.502	2.5474	-8.7533	-0.9911	-2.9699	-5.8891	-1.7796
G+Q+EX2	-16.473	0.4217	2.1592	6.8381	4.5809	-8.4962	-0.8773	-2.9571	-5.7653	-1.7749
G+Q+EY1	-26.2191	-5.5856	-0.693	1.9693	-14.1353	-10.658	-1.6476	-2.9846	-5.1369	-1.698
G+Q+EY2	-24.3029	-4.211	-1.0694	-3.7912	-10.9444	-10.236	-1.4615	-2.9674	-4.9715	-1.6962
G+Q-EX1	-19.002	-0.5947	-4.0105	-9.3649	-5.3447	-8.8902	-0.7288	-2.6494	-2.6065	-1.0605
G+Q-EX2	-20.1737	-1.4296	-3.7762	-8.701	-7.3782	-9.1474	-0.8425	-2.6623	-2.7303	-1.0652
G+Q-EY1	-10.4276	4.5777	-0.9241	-3.8322	11.338	-6.9856	-0.0723	-2.6348	-3.3587	1.1422
G+Q-EY2	-12.3437	3.2031	-0.5476	1.9283	8.1471	-7.4071	-0.2583	-2.652	-3.5241	-1.144

Table 3. End forces for S41 column.

Load	Ni	V2i	V3i	M2i	M3i	Nj	V2j	V3j	M2j	M3j
Unit	kN	kN	kN	kNm	kNm	kN	kN	kN	kNm	kNm
G+Q+EX1	-48.7032	0.7899	2.8457	7.027	-3.8821	3.1913	-0.1367	0.0842	-0.0021	0.0024
G+Q+EX2	-48.5319	0.9015	2.7247	6.7085	5.0593	3.187	-0.1367	0.0792	-0.0019	0.0024
G+Q+EY1	**-52.8743**	-4.375	0.2716	2.4961	-13.3664	3.2735	-0.0689	-0.0084	0.0018	0.0013
G+Q+EY2	-52.7482	-4.1513	0.0898	2.0797	-12.8567	**3.275**	-0.0736	-0.0125	0.0019	0.0015
G+Q-EX1	-49.3692	0.9242	-2.7437	-6.848	4.9191	3.2652	-0.1009	-0.0863	**0.0034**	0.0011
G+Q-EX2	-49.5405	0.8126	-2.6227	-6.5295	-4.0223	3.2695	-0.1009	-0.0813	0.0033	0.0011
G+Q-EY1	-45.1981	**6.0891**	-0.1696	-2.3171	**14.4034**	3.1831	**-0.1687**	0.0063	-0.0004	0.0022
G+Q-EY2	-45.3242	5.8654	0.0122	-1.9008	13.8937	3.1816	-0.164	0.0101	-0.0005	0.002

When the S42 column was examined, it was observed that the largest normal force in *i* direction was -56.3 kN (Table 4). This value is larger than S41 column. This is because the S42 column is one of the main columns and the most critical columns that hold the balcony floor. The biggest shear force obtained in *i* direction is 6.62 kN. This value is greater than the shear force value obtained for S41 column, and this shear force value was obtained in the same combination with S41 column. The greatest moment value in the same direction is 16.11 kN. The largest normal force occurring in *j* direction is 5.66 kN. The greatest shear force obtained in the same direction is -0.21 kN. Finally, the largest moment value obtained on this column is -0.005 kNm.

Table 4. End forces for S42 column.

Load	Ni	V2i	V3i	M2i	M3i	Nj	V2j	V3j	M2j	M3j
Unit	kN	kN	kN	kNm	kNm	kN	kN	kN	kNm	kNm
G+Q+EX1	-51.4463	1.0572	2.9484	7.1131	5.383	**5.6668**	-0.1696	0.1437	-0.0009	-0.0046
G+Q+EX2	-52.9597	1.6198	2.8359	6.8063	6.925	5.6517	-0.1748	0.1382	-0.0008	-0.0047
G+Q+EY1	**-56.3155**	-4.9636	0.0737	2.2645	-15.614	5.6125	-0.071	0.0073	0.0008	-0.0013
G+Q+EY2	-55.6158	-4.0023	-0.1085	-2.2028	-13.1544	5.5996	-0.083	-0.0005	0.0009	-0.0015
G+Q-EX1	-50.6571	0.6009	-2.882	-6.9882	-4.8848	5.3883	-0.1179	-0.1129	0.0016	-0.0017
G+Q-EX2	-51.1437	0.0383	-2.7695	-6.6814	-6.4268	5.4034	-0.1127	-0.1073	0.0015	-0.0016
G+Q-EY1	-47.7879	**6.6217**	-0.0074	-2.1397	**16.1122**	5.4425	**-0.2164**	0.0237	-0.0001	**-0.005**
G+Q-EY2	-48.4876	5.6604	0.1749	2.3277	13.6516	5.4555	-0.2045	0.0315	-0.0002	-0.0048

Balcony beams are named KZ1, KZ2 and KZ3. Table 5 shows the maximum force values for 8 combinations of KZ1 beam. Fig. 12 shows the deflection values occurred in the beam under G and Q loads. When Table 5 is examined, it is seen that the maximum normal force values in *i* and *j* directions for KZ1 beam are 1.12 kN and 2.13 kN, respectively. The biggest shear force value in *i* direction is -0.99 kN and the biggest shear force in *j* direction is 4.61 kN. The maximum moment values in *i* and *j* directions are 0.92 kNm and -7.17 kNm, respectively. Also, the deflection behavior of this beam under G and Q loads is shown in Fig. 12. Under G loading, deflection value at 0 m is -3.37 mm and at 4.5 m deflection value is -0.45 mm. The biggest deflection value in the beam under Q loading is -0.45 mm (Fig. 12).

Table 5. End forces for KZ1 beam.

Load	Ni	V2i	V3i	M2i	M3i	Nj	V2j	V3j	M2j	M3j
Unit	kN	kN	kN	kNm	kNm	kN	kN	kN	kNm	kNm
G+Q+EX1	0.5186	-0.5063	-0.1428	-0.0825	0.7007	-1.8608	**4.6131**	0.043	0.2804	**-7.1787**
G+Q+EX2	0.4959	-0.5338	-0.1418	-0.0819	0.6893	-1.7843	4.5606	0.0359	0.2762	-7.0227
G+Q+EY1	1.076	-0.4052	-0.2673	-0.1702	0.9146	0.348	4.611	-0.1142	0.3498	-6.9812
G+Q+EY2	0.6283	-0.4371	-0.2776	-0.192	**0.9232**	0.8566	4.4986	-0.1254	0.3463	-6.721
G+Q-EX1	1.1049	-0.8919	-0.2009	-0.1378	-0.0362	**2.1338**	3.7048	-0.39	0.3268	-3.7176
G+Q-EX2	**1.1276**	-0.8644	-0.2019	-0.1383	-0.0248	2.0573	3.7573	-0.3829	0.3311	-3.8736
G+Q-EY1	0.5475	**-0.993**	-0.0764	-0.05	-0.2501	-0.075	3.7069	-0.2328	0.2574	-3.9151
G+Q-EY2	0.9953	-0.9611	-0.0661	-0.0283	-0.2587	-0.5836	3.8193	-0.2216	0.261	-4.1753

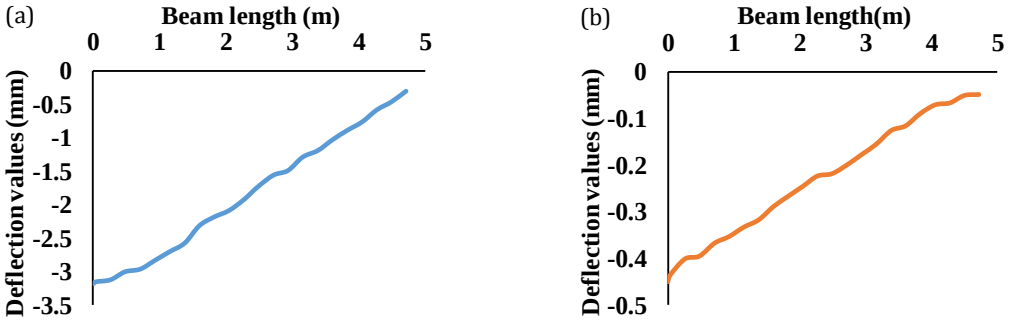

Fig. 12. Deflection values for KZ1 beam: (a) Under G loading; (b) Under Q loading.

When Table 6 is examined, force values are seen for KZ2 beam. The largest normal forces occurred in the KZ2 beam in *i* and *j* directions are 4.06 kN and 1.47 kN, respectively. In addition, the largest shear force value in *i* direction is -5.05 kN and the largest shear force in *j* direction is 1.49 kN. Besides, the greatest moment values in *i* and *j* directions are -8.11 kNm and 1.02 kNm (Table 6). Moreover, deflection values of this beam in G and Q loads are presented in Fig.13. The maximum deflection value occurred in the beam under G loading is -4.01 mm and this value occurred in the middle parts of the beam. In Q loading, the biggest deflection value occurred right in the middle of the beam and the deflection value is -0.61 mm. Finally, when the KZ3 beam is examined, it is seen that the largest shear force values in *i* and *j* directions are -2.07 kN and 1.88 kN, respectively (Table 7). In addition, the largest moment values in *i* and *j* directions were determined to be -1.33 kNm and -0.48 kNm. In Fig. 14, the biggest deflection values of the KZ3 beam under G and Q loads are presented. The largest deflection obtained in beam under G loading is -3.4 mm and this value occurred at the ends of the beam. The biggest deflection value acquired in the beam under Q loading is -0.46 mm.

Table 6. End forces for KZ2 beam.

Load	Ni	V2i	V3i	M2i	M3i	Nj	V2j	V3j	M2j	M3j
Unit	kN	kN	kN	kNm	kNm	kN	kN	kN	kNm	kNm
G+Q+EX1	**4.0688**	-3.2688	0.0788	0.1044	-2.2957	**1.4731**	**1.4986**	0.1147	-0.0387	-0.3564
G+Q+EX2	3.8195	-3.2798	0.1373	0.118	-2.3929	1.4365	1.4941	0.1027	-0.0303	-0.4146
G+Q+EY1	1.7387	-4.5999	-0.5744	0.1131	-6.7931	0.7974	0.7443	0.2079	-0.1501	**1.0271**
G+Q+EY2	1.3104	-4.6218	-0.4578	0.1427	-6.9585	0.4713	0.7419	0.1958	-0.1386	0.9242
G+Q-EX1	-1.3995	**-5.0542**	-0.1308	0.3456	**-8.1118**	-0.3083	0.5638	0.0703	-0.0981	0.8377
G+Q-EX2	-1.1503	-5.0432	-0.1893	0.332	-8.0145	-0.2717	0.5682	0.0823	-0.1065	0.8959
G+Q-EY1	0.9305	-3.7231	0.5224	0.3369	-3.6144	0.3674	1.318	-0.0229	-0.0133	-0.5458
G+Q-EY2	1.3588	-3.7011	0.4058	0.3072	-3.4489	0.6935	1.3204	-0.0108	-0.0018	-0.4429

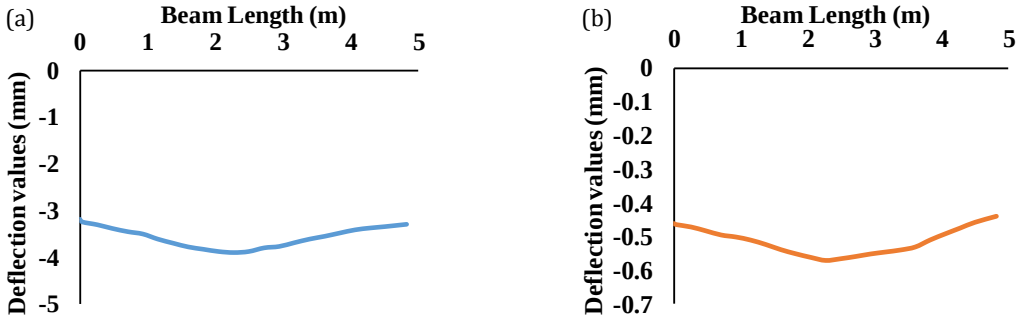

Fig. 13. Deflection values for KZ2 beam: (a) Under G loading; (b) Under Q loading.

Table 7. End forces for KZ3 beam.

Load	Ni	V2i	V3i	M2i	M3i	Nj	V2j	V3j	M2j	M3j
Unit	kN	kN	kN	kNm	kNm	kN	kN	kN	kNm	kNm
G+Q+EX1	**0.9482**	-1.9184	0.3348	0.1365	-0.5125	0.488	1.8541	-0.0748	-0.0285	-0.3113
G+Q+EX2	0.9471	-1.9459	0.3334	0.141	-0.9508	0.4461	1.834	-0.0833	-0.0265	-0.2869
G+Q+EY1	0.3691	-1.846	0.2175	0.0309	-0.1181	0.8361	1.8156	-0.1527	-0.0376	0.3567
G+Q+EY2	0.088	-1.9083	0.2219	0.0411	-0.2706	0.2988	1.7885	-0.1656	-0.0415	0.4227
G+Q-EX1	-0.3304	-1.999	0.1828	0.0506	-0.9361	0.6726	1.8175	-0.3315	0.0624	0.2476
G+Q-EX2	-0.3293	-1.9715	0.1843	0.0461	-0.4978	0.7153	1.8375	-0.323	0.0605	0.2231
G+Q-EY1	0.2487	**-2.0714**	0.3002	0.1562	**-1.3305**	0.3253	1.856	-0.2535	0.0715	-0.4205
G+Q-EY2	0.5298	-2.0091	0.2957	0.146	-1.178	0.8626	**1.883**	-0.2407	0.0755	**-0.4865**

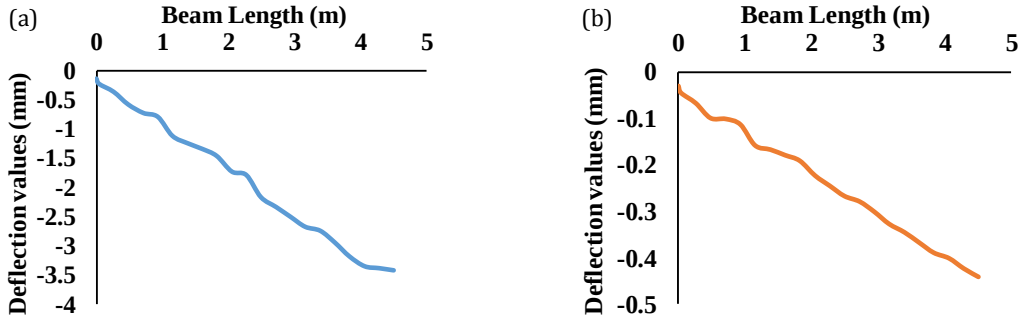

Fig. 14. Deflection values for KZ3 beam: (a) Under G loading; (b) Under Q loading.

5.2. Analysis results for situation after strengthening

The reinforcement was carried out on damaged carrier elements for the current situation of the building, and this was applied to 4 balcony main columns. In this section, the maximum force values obtained after reinforcement for 4 main columns and 3 balcony beams are presented. Table 8 shows the maximum forces for the S40 column. As can be seen from Table 8, the big-gest normal force affecting the column is -35.6 kN in *i* direction and 23.1 kN in *j* direction. When these values are compared with the currently obtained values, it can be seen that the S40 column can carry more normal force after reinforcement. When the largest shear forces occurred in *i* and *j* directions are examined, it is seen that the maximum shear force in *i* direction is 10.24 kN and in *j* direction it is 10.27 kN. When the current analysis results and post-reinforcement analysis results are examined, it is concluded that the columns can carry more shear force after reinforcement. Finally, when the largest moment values in *i* and *j* directions are examined, it is seen that the moment values are 30.46 kNm and 10.3 kNm, respectively (Table 8).

The end force values of S39 column under 8 load combinations are presented in Table 9. When Table 9 is examined, it is seen that the load and moment values that the S39 column can carry are close to the load and moment values that the S40 column can carry. The greatest normal force values occurring in *i* and *j* directions are -36.9 kN and -17.5 kN, respectively. In addition, the largest shear force values occurring in *i* and *j* directions are -10.02 kN and -3.55 kN, respectively. It is concluded that for the S39 column, the normal force and shear forces obtained after reinforcement are higher than the normal force and shear forces obtained. Finally, it is seen that the maximum moment values that the column can carry *i* and *j* directions are much larger after reinforcement (Table 9).

Table 8. End forces for S40 column.

Load	Ni	V2i	V3i	M2i	M3i	Nj	V2j	V3j	M2j	M3j
Unit	kN	kN	kN	kNm	kNm	kN	kN	kN	kNm	kNm
G+Q+EX1	-24.9408	**10.2401**	2.67	15.1234	**30.4665**	14.5928	**10.2725**	-1.1492	-2.1116	**10.3**
G+Q+EX2	-25.7792	9.6012	3.5366	17.3775	28.5153	15.0945	9.5511	-1.3727	-2.8172	9.8458
G+Q+EY1	-34.2425	0.5635	7.3494	22.1163	-5.4131	21.2956	1.2501	-3.425	-1.8632	-1.6568
G+Q+EY2	**-35.614**	-0.505	8.8625	26.1148	-8.7449	22.0898	0.0396	-3.8044	-3.1088	-2.4848
G+Q-EX1	-31.6792	-8.2347	-1.4106	-11.6412	-27.1047	**23.1024**	-7.0087	-0.8044	5.3134	-7.0174
G+Q-EX2	-30.8408	-7.5958	-2.2772	-13.8953	-25.1535	22.6008	-6.2872	-0.6172	6.0191	-6.5631
G+Q-EY1	-22.3775	1.4419	-6.09	-18.6341	8.7749	16.3996	2.0137	1.435	5.065	4.9395
G+Q-EY2	-21.006	2.5104	-7.6031	-22.6325	12.1067	15.6055	3.2242	1.8144	6.3106	5.7674

Table 9. End forces for S39 column.

Load	Ni	V2i	V3i	M2i	M3i	Nj	V2j	V3j	M2j	M3j
Unit	kN	kN	kN	kNm	kNm	kN	kN	kN	kNm	kNm
G+Q+EX1	-26.6655	3.5962	7.8924	28.9874	17.9951	-13.6691	-2.9335	-3.3922	-7.0787	-9.1926
G+Q+EX2	-25.4067	5.669	7.4203	27.2472	24.578	-13.2283	-2.8526	-3.4379	-7.1503	-9.6613
G+Q+EY1	**-36.9216**	-9.9872	-1.6869	-8.7823	-41.067	**-17.592**	**-3.5511**	-3.1639	-2.0658	-6.4892
G+Q+EY2	-34.8039	-6.4941	-2.4541	-11.7044	-30.1029	-16.8455	-3.4126	-3.2347	-2.1687	-7.274
G+Q-EX1	-32.2685	-6.1465	-10.0284	-31.3217	-30.3015	-15.2505	-0.4679	-2.8166	-0.0211	2.5691
G+Q-EX2	-33.5272	-8.2193	-9.5564	-29.5815	-36.8843	-15.6913	-0.5489	-2.771	0.0505	3.0377
G+Q-EY1	-22.0123	7.4369	-0.4492	6.448	28.7607	-11.3276	0.1497	-3.045	-5.034	-0.1344
G+Q-EY2	-24.13	3.9438	0.3181	9.3701	17.7966	-12.0741	0.0112	-2.9742	-4.9311	0.6505

According to Table 10, the biggest normal forces occurred on the S41 column for *i* and *j* directions are -65.01 kN and 32.77 kN, respectively. Moreover, the largest shear force took place in *i* direction is 12.95 kN and -3.81 kN in *j* direction. The maximum moment values in *i* and *j* directions for the S41 column are -44.14 kNm and 5.96 kNm (Table 10), respectively. These values are much larger than force values obtained for current situation. This result is an indication that strengthening and historical structures can carry more strength and survive more. When Table 11 is examined, the end forces and moments of S42 column are seen. When com-pared with S41 column, it is seen that S42 column can carry similar loads and moments. The largest normal forces occurred in *i* and *j* directions are -67.35 kN and 34.52 kN, respectively. In addition, the largest shear force value in *i* direction is 10.86 kN and 5.84 kN in *j* direction. Finally, the largest moment for *i* and *j* directions are -42.18 kNm and 4.97 kNm, respectively.

Table 10. End forces for S41 column.

Load	Ni	V2i	V3i	M2i	M3i	Nj	V2j	V3j	M2j	M3j
Unit	kN	kN	kN	kNm	kNm	kN	kN	kN	kNm	kNm
G+Q+EX1	-61.6509	-0.25	8.5475	26.986	-20.3559	31.8096	-2.4216	3.6752	5.2608	4.8879
G+Q+EX2	-61.5739	-0.6433	8.5353	26.7604	-21.1942	31.8737	-2.667	3.6068	5.6704	5.6919
G+Q+EY1	-65.1565	-10.3567	-0.0281	6.6646	-42.5935	32.6335	-1.0561	0.0984	1.7837	4.5999
G+Q+EY2	**-65.0191**	-11.0301	0.0095	6.3548	**-44.1465**	**32.7707**	-1.5781	0.0077	2.3997	**5.9697**
G+Q-EX1	-60.4007	2.175	-8.8615	-27.3627	16.383	29.7635	-2.4401	**-3.8171**	0.8604	0.3315
G+Q-EX2	-60.4777	2.5682	-8.8492	-27.1371	17.2213	29.6994	-2.1947	-3.7487	0.4508	-0.4726
G+Q-EY1	-56.8951	12.2817	-0.2858	-7.0413	38.6206	28.9397	-3.8056	-0.2403	4.3375	0.6194
G+Q-EY2	-57.0325	**12.9551**	-0.3234	-6.7315	40.1736	28.8025	-3.2836	-0.1496	3.7215	-0.7504

Table 11. End forces for S42 column.

Load	Ni	V2i	V3i	M2i	M3i	Nj	V2j	V3j	M2j	M3j
Unit	kN	kN	kN	kNm	kNm	kN	kN	kN	kNm	kNm
G+Q+EX1	-62.8816	2.9726	8.5852	26.83	16.7672	32.8466	-0.9902	**5.8495**	4.5431	0.4245
G+Q+EX2	-62.5615	3.864	8.5956	26.6401	20.1994	32.7544	-1.2195	5.8155	**4.9761**	0.6165
G+Q+EY1	**-67.3568**	-8.8745	-0.1915	6.381	**-42.1887**	**34.529**	1.1498	1.4108	3.4787	0.1533
G+Q+EY2	-66.917	-7.2738	-0.1774	-6.7407	-36.3103	34.3787	0.7355	1.3982	4.2231	0.4709
G+Q-EX1	-63.9995	-0.983	-8.7864	-27.1143	-22.7481	33.1155	-1.8639	-3.0975	1.4281	3.7528
G+Q-EX2	-64.3196	-1.8743	-8.7969	-26.9244	-26.1802	33.2077	-1.6346	-3.0635	0.9951	3.5608
G+Q-EY1	-59.5243	**10.8642**	-0.0098	-6.6653	36.2079	31.4331	-4.0039	1.3413	2.4926	4.024”
G+Q-EY2	-59.964	9.2635	-0.0238	6.4563	30.3295	31.5834	-3.5895	1.3538	1.7482	3.7064

Table 12 presents the end forces for the KZ1 beam. The largest normal force value in *i* direction affecting the beam is 1.81 kN. In addition, the largest normal force in *j* direction is 3.85 kN. The greatest moment value in *i* direction is -0.78 kNm and the greatest moment value in *j* direction is -7.36 kNm. In Fig. 15, deflection values took place in the beam under G and Q loading are presented graphically. Under G loading, deflection value of -0.1 mm occurred in the beam at 0 m. However, deflection of -1.61 mm took place at the end of the beam (4.7 m) (Fig. 15a). Under Q loading, the maximum deflection occurred at the ends of the beam and its value is -0.27 mm (Fig. 15b).

Table 12. End forces for KZ1 beam.

Load	Ni	V2i	V3i	M2i	M3i	Nj	V2j	V3j	M2j	M3j
Unit	kN	kN	kN	kNm	kNm	kN	kN	kN	kNm	kNm
G+Q+EX1	0.7922	-0.6835	-0.0651	-0.0198	0.419	-2.8833	4.642	0.3589	0.0992	**-7.3611**
G+Q+EX2	0.5136	-0.7055	-0.0765	-0.1169	0.4208	-2.9764	4.5906	0.3961	0.0869	-7.2328
G+Q+EY1	-0.0223	-0.6944	-0.2103	-0.1482	0.437	0.5966	4.254	0.1622	0.1935	-6.6254
G+Q+EY2	-0.4492	-0.714	-0.3269	-0.1882	0.4403	0.7894	4.1444	0.2376	0.1691	-6.3903
G+Q-EX1	0.5737	-1.1491	-0.1801	-0.1175	-0.758	3.7651	3.1172	-0.86	0.5257	-2.9859
G+Q-EX2	0.8523	-1.1271	-0.1688	-0.0204	-0.7597	**3.8582**	3.1686	-0.8972	0.5381	-3.1142
G+Q-EY1	1.3882	-1.1382	-0.0349	0.011	-0.7759	0.2851	3.5052	-0.6633	0.4315	-3.7216
G+Q-EY2	**1.8151**	-1.1186	0.0817	0.0509	**-0.7792**	0.0924	3.6149	-0.7387	0.4559	-3.9567

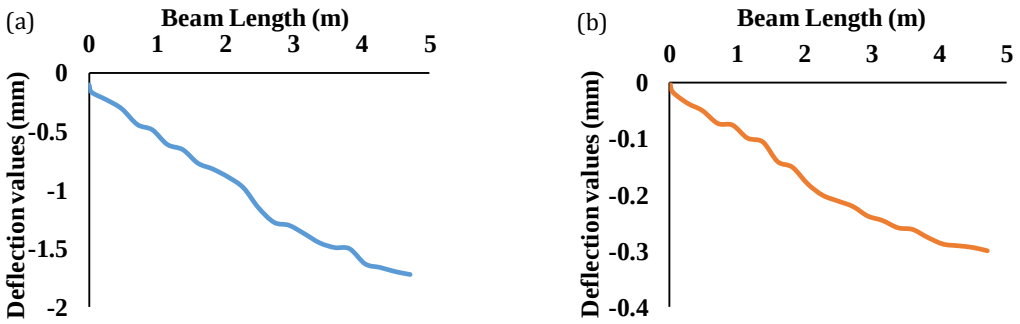

Fig. 15. Deflection values for KZ1 beam: (a) Under G loading; (b) Under Q loading.

In Tables 13 and 14, force values are presented for 8 different combinations for KZ2 and KZ3 beams. According to Table 13, maximum normal force of 2.41 kN occurred for G+Q+EX loading in *i* direction in the KZ2 beam. In *j* direction, 1.93 kN normal force was obtained. In addition, the maximum shear forces in *i* and *j* directions are 2.04 kN and 1.98 kN, respectively. Finally, the maximum moment values in *i* and *j* directions are -1.53 kNm and -0.87 kNm, respectively (Table 13). Also, deflection values occurred under G and Q loads in KZ2 beam are presented in Fig. 16. According to Fig. 16, maximum deflection took place in the middle parts of the beam under G loading and its numerical value is -2.12 mm. Under Q loading, the maximum deflection is similarly observed in the middle parts of the beam and its numerical value is -0.4 mm.

Table 14 presents the maximum force values for the KZ3 beam. The largest normal forces occurred in *i* and *j* directions are 9.45 kN and 3.05 kN, respectively. Considering 8 different combinations in this beam, the largest

shear force value is -4.95 kN in the *i* direction and 1.6 kN in the *j* direction. Finally, the greatest moment values in the KZ3 beam in *i* and *j* directions are -7.51 kNm and -1.09 kNm, respectively. Deflection values under G and Q loads for KZ2 beam are presented in Fig. 17. The maximum deflection for G loading occurred at the ends of the beam and its value is -1.58 mm. In addition, the biggest deflection value for Q loading is -0.28 mm. In addition, in Table 15, deflection values occurred in beams before and after reinforcement were compared and tabulated. As can be seen from Table 15, earthquake reinforcement in historical buildings reduces deflection values in beams.

Table 13. End forces for KZ2 beam.

Load	Ni	V2i	V3i	M2i	M3i	Nj	V2j	V3j	M2j	M3j
Unit	kN	kN	kN	kNm	kNm	kN	kN	kN	kNm	kNm
G+Q+EX1	**2.4181**	-1.9981	0.4074	0.193	-0.9261	0.9735	1.8793	0.0266	-0.0506	-0.6934
G+Q+EX2	2.2173	-2.0239	0.4006	0.1947	-1.2984	0.6584	1.8596	0.0322	-0.0539	-0.659
G+Q+EY1	0.1875	-1.9251	0.1841	0.0478	-0.719	-0.12	1.8267	0.0518	-0.0656	-0.0582
G+Q+EY2	-0.4105	-1.9848	0.1805	0.0538	-0.8555	-0.7814	1.8084	-0.0529	-0.0519	0.0111
G+Q-EX1	-1.3955	-1.9729	0.0873	0.0364	-1.3241	0.1803	1.9137	-0.27	0.1006	-0.1746
G+Q-EX2	-1.1947	-1.9471	0.0941	0.0347	-0.9518	0.4954	1.9334	-0.2756	0.1039	-0.2089
G+Q-EY1	0.8352	**-2.0458**	0.3105	0.1815	**-1.5312**	1.2738	1.9663	-0.2952	0.1156	-0.8098
G+Q-EY2	1.4331	-1.9861	0.3141	0.1755	-1.3947	**1.9352**	**1.9846**	-0.1904	0.1019	**-0.879**

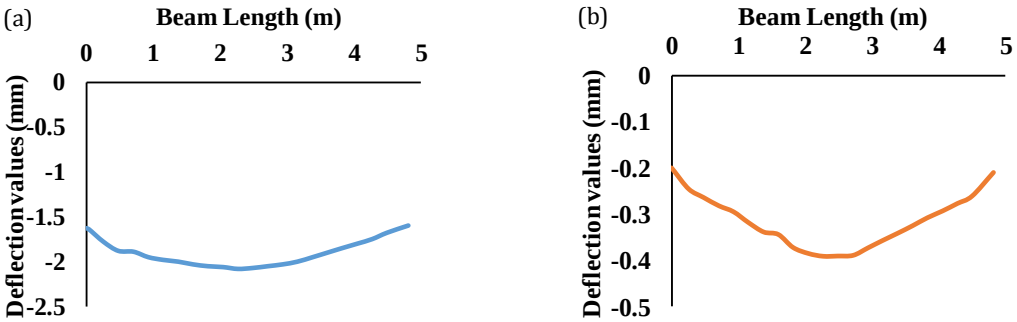

Fig. 16. Deflection values for KZ2 beam: (a) Under G loading; (b) Under Q loading.

Table 14. End forces for KZ3 beam.

Load	Ni	V2i	V3i	M2i	M3i	Nj	V2j	V3j	M2j	M3j
Unit	kN	kN	kN	kNm	kNm	kN	kN	kN	kNm	kNm
G+Q+EX1	**9.4559**	-3.1857	1.4965	0.6483	-2.666	**3.0547**	1.6025	0.107	0.0095	-1.0472
G+Q+EX2	8.9764	-3.17	1.8195	0.7214	-2.6935	2.8082	**1.6056**	0.0944	0.0172	**-1.0932**
G+Q+EY1	1.0484	-4.5252	-1.7616	-0.2927	-6.5348	0.4798	0.9807	0.1748	-0.0971	0.3714
G+Q+EY2	0.2457	-4.501	-1.1794	-0.1571	-6.5827	-0.1855	0.9929	0.1579	-0.0857	0.2851
G+Q-EX1	-6.3024	-4.9345	-1.6016	-0.24	**-7.5151**	-1.6796	0.8938	-0.0319	-0.04966	0.4676
G+Q-EX2	-5.8229	**-4.9502**	-1.9246	-0.3131	-7.4882	-1.4331	0.8907	-0.0192	-0.0573	0.5137
G+Q-EY1	2.1051	-3.595	1.6565	0.701	-3.6469	0.8953	1.5156	-0.0997	0.0571	-0.951
G+Q-EY2	2.9078	-3.6192	1.0743	0.5653	-3.599	1.5606	1.5033	-0.0828	0.0456	-0.8646

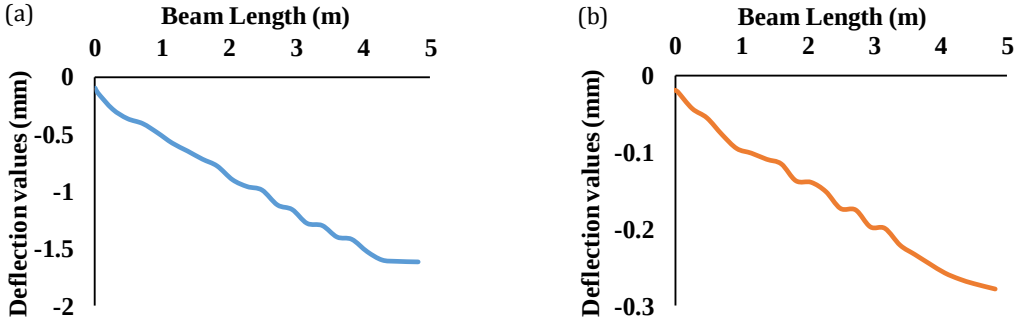

Fig. 17. Deflection values for KZ3 beam: (a) Under G loading; (b) Under Q loading.

Table 15. Deflection values in beams before and after reinforcement.

Beam Name	KZ1		KZ2	KZ3	
Length	0 m	0.45 m	Middle point	0 m	0.45 m
Deflection Before Strengthening (mm)	-0.45	-3.37	-4.01 mm	-0.25 mm	-3.4 mm
Deflection After Strengthening (mm)	-0.1 mm	-1.61 mm	-2.12 mm	-0.15 mm	-1.58 mm

6. Conclusions

In this study, it is aimed to determine how important the jacketing is for earthquake safety and service life of historical buildings. For this purpose, Zonguldak historical cinema building was selected for 3D modeling in this study. After the building was modelled as three dimensional, current situation of building was analyzed by using IDECAD program. Later, it was ensured that the building survived for a long time by using jacketing method. According to analysis results, jacketing behaviour of concrete historical building is evaluated as below.

- Strengthening historical structures by using jacketing is great importance for safety and future of these structures. During jacketing process, great care should be taken thickness and location of jacketing.
- During strengthening of historical buildings, care should be taken to consider the damaged areas that were determined by using 3D modeling and 3D analyzing.
- When compared the current situation of building and strengthened situation of building, it is clearly observed that the moments and shear forces resisted to demolition are higher after strengthening for balcony beams.
- According to the 2018 Turkish earthquake code, although the collapse damage zone was obtained for RC building before strengthening, limited damage zone was obtained after strengthening.
- When compared before and after strengthening process, it was clearly seen that more deflections occurred in balcony beams before strengthening and that these deflection values decreased after strengthening.
- The moments of the columns and beams after strengthening have significantly increased due to the increased rigidity by jacketing. This result is an indication that historical structures can carry more strength and moment and survive more with jacketing.

References

Aigwi IE, Egbelakin T, Ingham J, Phipps R, Rotimi J, Filippova O (2019). A performance-based framework to prioritise underutilised historical buildings for adaptive reuse interventions in New Zealand. *Sustainable Cities and Society*, 48, 101547.

Arıoğlu E, Anadol K, Arıoğlu AÜ (2007). Uluslararası deprem mühendisliği açısından önemli bir olgu ve kayıp: "Güçlendirilmiş Adapazarı Vilayet Binası". *Tarihi Eserlerin Güçlendirilmesi ve Geleceğe Güvenle Devredilmesi Sempozyumu*, 27-29 September 2007, 241-254.

Aydın AP, Kul FN, Dönmez C, Erberik A (2015). Urla eski Tekel Binası (Arditi Köşkü): Yangın öncesi durum ve yapısal iyileştirme-güçlendirme kararları. *5. Tarihi Eserlerin Güçlendirilmesi ve Geleceğe Güvenle Devredilmesi Sempozyumu*, 1-3 October 2015, 13-28.

Cakir F, Uckan E, Shen J, Seker BS, Akbas B (2015). Seismic damage evaluation of historical structures during Van earthquake, October 23, 2011. *Engineering Failure Analysis*, 58, 249-266.

Ercan E (2018). Assessing the impact of retrofitting on structural safety in historical buildings via ambient vibration tests. *Construction and Building Materials*, 164, 337-349.

Günaydın M (2019). Seismic performance evaluation of a fire-exposed historical structure using an updated finite element model. *Engineering Failure Analysis*, 106, 104149.

Karaton M, Aksoy HS, Sayın E, Calayır Y (2017). Nonlinear seismic performance of a 12th century historical masonry bridge under different earthquake levels. *Engineering Failure Analysis*, 79, 408-421.

Kasapgil M (2007). Adana Ulucami minaresi güçlendirme çalışması. *Tarihi Eserlerin Güçlendirilmesi ve Geleceğe Güvenle Devredilmesi Sempozyumu*, 27-29 September 2007, 219-224.

Kasapgil ME (2007). Eski eserlerde, yığma duvarların, kubbelerin, tonozların ve temellerin enjeksiyon reçineleri ve ankraj sistemleriyle güçlendirilmesi. *Tarihi Eserlerin Güçlendirilmesi ve Geleceğe Güvenle Devredilmesi Sempozyumu*, 27-29 September 2007, 215-218.

Korkmaz M, Ozdemir MA, Kavali E, Cakir F (2018). Performance-based assessment of multi-story unreinforced masonry buildings: The case of historical Khatib School in Erzurum, Turkey. *Engineering Failure A*nalysis, 94, 195-213.

Mahrebel HA (2006). Tarihi Yapılarda Taşıyıcı Sistem Özellikleri, Hasarlar, Onarım ve Güçlendirme Teknikleri. *M.Sc. thesis*, İstanbul Technical University, Turkey.

Onat O, Sayın E (2015). Tarihi Tağar Köprüsünün doğrusal olmayan sismik analizi. *5. Tarihi Eserlerin Güçlendirilmesi ve Geleceğe Güvenle Devredilmesi Sempozyumu*, 1-3 October 2015, 301-311.

Orhan S, Özyazıcıoğlu MH (2015). Determination of collapse load of single span circular masonry arch bridges by the methods of limit analysis. *Pamukkale University Journal of Engineering Sciences*, 21(3), 88-93.

Örmecioğlu HT (2010). Tarihi yapıların yapısal güçlendirilmesinde ana ilkeler ve yaklaşımlar. *Journal of Polytechnic*, 13(3), 233-237.

Sert H, Partal EM (2015). Tarihi köprülerin restorasyonları kapsamında yürütülen yapısal analiz çalışmaları ve sonuçları. *5. Tarihi Eserlerin Güçlendirilmesi ve Geleceğe Güvenle Devredilmesi Sempozyumu,* 1-3 October 2015, 83-97.

Sert H, Yılmaz S (2015). Tarihi Malabadi (Batman Su) Köprüsü'nde yürütülen restorasyon-konservasyon çalışmaları. *5. Tarihi Eserlerin Güçlendirilmesi ve Geleceğe Güvenle Devredilmesi Sempozyumu*, 1-3 Ekim 2015, s.143-153.

Sesigür H, Çelik OC (2007). Ahi Çelebi Camisinin onarımı ve güçlendirilmesi. *Tarihi Eserlerin Güçlendirilmesi ve Geleceğe Güvenle Devredilmesi Sempozyumu*, 27-29 September 2007, 231-238.

Türker T, Bayraktar A, Kocaman İ, Çoruhlu B (2015). Ölçekli yığma taş kemer köprü modelinin dinamik davranışının deneysel ve analitik olarak incelenmesi. *5. Tarihi Eserlerin Güçlendirilmesi ve Geleceğe Güvenle Devredilmesi Sempozyumu*, 1-3 October 2015, 113-126.

Valente M, Milani G (2019). Damage assessment and collapse investigation of three historical masonry palaces under seismic actions. *Engineering Failure Analysis*, 98, 10-37.